

Contents

Abstract (Chinese)	I
Abstract (English)	III
Acknowledgements	VI
Contents	VII
Figure Captions	IX

Chapter 1

Introduction	1
1.1 Overview of Organic Thin Film Transistors and Active-Matrix Pixel for Novel display Applications.....	1
1.1.1 The Basic Operation Mode and Principles of Organic Thin Film Transistors.....	3
1.1.2 The Carrier Transport in Organic Semiconductors.....	6
1.1.3 The structures of Pentacene.....	8
1.2 Motivation.....	10
1.3 Thesis outlines.....	12

Chapter 2

The Study on Polycrystalline Pentacene Thin Film Transistors	19
2.1 Introduction.....	19
2.2 Experiment	20
2.3 Result and Discussion.....	22
2.3.1 The Growth of Pentacene.....	22
2.3.2 Comparison of Top Contact and Bottom Contact Configurations.....	25
2.3.3 V_{th} Model Proposed by R. Schroeder.....	27
2.3.4 Space-Charge Limited Current in Linear Region.....	29
2.3.5 Pentacene Bulk Traps dependent V_{th} Model.....	31
2.4 Conclusion.....	33

Chapter 3

Atmosphere Effect on Pentacene Thin Film Transistors	50
3.1 Introduction.....	50
3.2 Experiment.....	51
3.3 Grain Boundary Potential Barrier Model.....	52
3.4 Result and Discussion.....	53
3.4.1 Atmosphere Effect on Top Contact Configuration.....	54

3.4.2 Atmosphere Effect on Field Effect Mobility.....	55
3.4.3 Trap Density Extracted by Levinson Model.....	57
3.4.4 Atmosphere Effect on Bottom Contact Configuration.....	59
3.5 Conclusion.....	62

Chapter 4

The Driving of Liquid Crystal Display by Pentacene Thin Film Transistors.....73

4.1 Introduction.....	73
4.2 Experiment.....	74
4.3 Result and Discussion.....	75
4.3.1 Sensitivity to Humidity.....	75
4.3.2 Effect of Passivation Layer.....	76
4.3.3 The Illumination Effect.....	77
4.3.4 The Uniformity in Local Substrate.....	77
4.3.5 Gate Bias Stress.....	78
4.3.6 The Driving of Display.....	80
4.4 Conclusion.....	82

Chapter 5

The Active-Matrix Pixel Structure Application in Field Emission Display.....96

5.1 Introduction.....	96
5.2 Experiment.....	97
5.3 Result and Discussion.....	98
5.3.1 The Proposed Novel Pixel Structure.....	98
5.3.2 The Characteristics of Carbon Nanotube Field Emission Display...	100
5.3.3 The Driving Requirement and Result of Active-Matrix Field Emission Display.....	100
5.4 Conclusion.....	102

Chapter 6

Conclusions and Further Recommendations.....113

6.1 Conclusions.....	113
6.2 Further Recommendation.....	115

References.....118

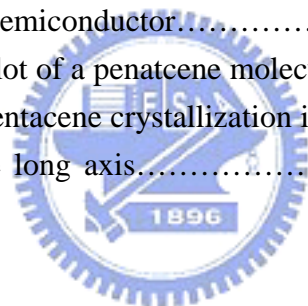
Vita

Publication List

Figure captions

Chapter 1

- Fig. 1.1 (a) Cross section view of inverted staggered type organic TFTs. (b) Cross section view of inverted coplanar type organic TFTs.....14
- Fig. 1.2 (a) Schematic of operation of organic TFTs, showing a lightly p-doped semiconductor; + indicates a positive charge; \ominus indicates a negative charge. (b) Development of a positive accumulation layer when a negative gate bias is applied. (c) Development of a depletion region when a negative gate bias is applied.....15
- Fig. 1.3 The properties of an inverted coplanar pentacene TFT utilizing ITO as electrodes with channel width 10000 μm and channel length 57 μm . (a) The transfer curve of $V_D = -50$ V. (b) The output curves.....16
- Fig. 1.4 The energy band diagram shows the formation of LUMO (Lowest Unoccupied Molecular Orbital) and HOMO (Highest Occupied Molecular Orbital) in organic semiconductor.....17
- Fig. 1.5 (a) The schematic plot of a pentacene molecules. (b) The crystal structure of the layer by layer pentacene crystallization in the direction of [110] axis. (c) Top view along the long axis.....18



Chapter 2

- Fig. 2.1 The vacuum thermal evaporation system for pentacene.....34
- Fig. 2.2 The fabrication process flow of inverted staggered type pentacene TFTs with Au as contact electrodes.....35
- Fig. 2.3 The fabrication process flow of inverted coplanar type pentacene TFTs with ITO as contact electrodes.....36
- Fig. 2.4 The pentacene growth on silicon dioxide with different substrate temperatures of (a) room temperature, (b) 50 $^{\circ}\text{C}$, (c) 70 $^{\circ}\text{C}$, and (d) 90 $^{\circ}\text{C}$, respectively.....37
- Fig. 2.5 The pentacene growth on oxide with different surface treatment layer (a) without any pretreatment, just only oxide, (b) with HMDS treatment, (c) with a layer of polyimide, all with substrate temperature 70 $^{\circ}\text{C}$, respectively.....38
- Fig. 2.6 (a) The X-ray diffraction plot of Fig. 2.5(a)(c) samples, pentacene was grown on oxide or polyimide layer, respectively. (b) The enlargement and analysis of (a).....39

Fig. 2.7	The properties of an inverted coplanar pentacene TFT utilizing ITO as electrodes with channel width 500 μm and channel length 37 μm . (a) The transfer curve of $V_D = -100$ V. (b) The output curves.....	40
Fig. 2.8	The properties of an inverted staggered pentacene TFT utilizing Au as electrodes with channel width 1000 μm and channel length 100 μm . (a) The transfer curve of $V_D = -100$ V. (b) The output curves.....	41
Fig. 2.9	The surface morphology of pentacene on an inverted coplanar type TFT utilizing ITO as electrodes, (a) pentacene on ITO electrode, (b) pentacene on the junction of ITO electrode and channel oxide region, and (c) pentacene on the oxide channel region.....	42
Fig. 2.10	(a) Schematic plot of cross section of inverted-staggered (top contact) device geometry (b) The corresponding cross section SEM image.....	43
Fig. 2.11	The top view SEM images of pentacene film with thickness of (a) very thin, (b) 65 nm, and (c) 106 nm, respectively, in the channel region.....	44
Fig. 2.11	The top view SEM images of pentacene film with thickness of (d)143 nm and (e)167 nm, respectively, in the channel region.....	45
Fig. 2.12	Transfer characteristics in (a) log scale and (b) double-log scale of four pentacene TFTs with different thickness: a-65 nm; b-106 nm; c-143 nm; d-167 nm.....	46
Fig. 2.13	Output characteristics in double-log scale at $V_G = -100$ V for the four pentacene TFTs with different thickness.....	47
Fig. 2.14	(a) Output characteristics in linear scale at $V_G = -100$ V for the four pentacene TFTs with different thickness. (b) Enlargement of (a) at small drain bias.....	48
Fig. 2.15	The threshold voltage as a function of thickness of pentacene layer. The threshold voltage was extracted by various methods. Lines are the numerical fits based on Eq. (2.3). Solid line and dashed line are fits for threshold voltage measured by square root method and CV method, respectively.....	49

Chapter 3

Fig. 3.1	Schematic diagram of (a) an inverted staggered pentacene transistor with gold top contact (TC TFT), (b) an inverted coplanar pentacene transistor with ITO bottom contact (BC TFT), (c) atomic force microscope image of thermally deposited pentacene film on SiO_2 surface in TC TFT, (d) pentacene film in BC TFT.....	63
Fig. 3.2	The Vacuum Measurement System.....	64

Fig. 3.3	Energy scheme of two cases of polycrystalline semiconductors, (a) The grain length, L , larger than twice depleted length, W_d , as $L > 2 W_d$. (b) $L < W_d$. E_b is the energy barrier height.	65
Fig. 3.4	I_D - V_{DS} characteristics of a TC pentacene transistor measured in air and in a vacuum. The V_G was varied from -20 V to -100 V with -20 V step.....	66
Fig. 3.5	$\text{Log}(I_D)$ - V_G (left-axis) and $(I_D)^{1/2}$ - V_G (right axis) characteristics of a TC pentacene transistors measured in air and in a vacuum with a V_{DS} of -100 V.....	66
Fig. 3.6	Variation of the field-effect motilities of a TC pentacene transistor as a function of $-(V_G - V_{th})$. Opened and closed symbols correspond to the data measured in air and in a vacuum, respectively.....	67
Fig. 3.7	Variation of the field-effect motilities of a TC pentacene transistor measured in a vacuum as a function of V_{DS} for $V_G = -100$ V, -80 V, -60 V, -40 V and -20 V.....	68
Fig. 3.8	The drain electric field dependence of the drift velocity of holes in TC pentacene transistor with a V_G of -100 V. The transistor was measured in air and then in a vacuum. The straight lines act as the reference.....	69
Fig. 3.9	Plot of $\ln(I_D/V_G)$ versus $(1/V_G)$ for a TC pentacene transistor measured in air and in a vacuum with a V_{DS} of -20 V.....	70
Fig. 3.10	(a) I_D - V_{DS} characteristics of a BC pentacene transistor measured in air and in a vacuum. The V_G was varied from -20 V to -100 V with -20 V step. (b) $\text{Log}(I_D)$ - V_G (left-axis) and $(I_D)^{1/2}$ - V_G (right axis) characteristics of a BC pentacene transistors measured in air and in a vacuum with a V_{DS} of -80 V.....	71
Fig. 3.11	Plot of $\ln(I_D/V_G)$ versus $(1/V_G)$ for a BC pentacene transistor measured in air and in a vacuum with a V_{DS} of -20 V.....	72

Chapter 4

Fig. 4.1	(a) The process flow of the inverted coplanar type pentacene TFTs.....	84
Fig. 4.1	(b) The process flow for an active matrix TNLC display driven by inverted coplanar type pentacene TFTs.....	85
Fig. 4.2	$\text{Log}(I_D)$ - V_G (left axis, open symbols) and $(I_D)^{1/2}$ - V_G (right axis, closed symbols) characteristics of a pentacene transistor measured in air (squares), in vacuum (circles), and in dry air after 25 hours of pre-test storage (triangles) with a V_{DS} of -50 V. The channel width and length are 20000 and 57 μm , respectively.....	86

Fig. 4.3 Measured output characteristics of a pentacene transistor. The triangle symbols indicate the bare device without any passivation layer. The circles indicate the same device with the PVA/PI passivation layer upon it. The square symbols show the same device with the PVA/PI passivation layer after the full cycle of liquid crystal processing. The curves correspond to five different gate–source biases, from -20 to -100 V, in increments of -20 V. The measurements were performed in ambient air condition. The featured device had a channel width and length of 500 and 50 μm , respectively.....**87**

Fig. 4.4 Transfer characteristics of a pentacene transistor under illumination (squares) and without illumination (circles). The curves correspond to two different V_{DS} of -10 V (closed symbols) and -50 V (open symbols), respectively. The measurements were performed in vacuum. The featured device had a channel width and length of 20000 and 57 μm , respectively.....**88**

Fig. 4.5 On current, off current, and threshold voltage of nine pentacene transistors distributed in a 3 inch organic TFTs array. The lines were drawn to guide to the eyes.....**89**

Fig. 4.6 The normalized drain current as a function of time of pentacene transistors stressed at V_G of -50 V and V_{DS} of -50 V in vacuum (squares) and in ambient air (circles).....**90**

Fig. 4.7 (a) The transfer curves, at V_{DS} of -50 V, in the conditions of the origin state, after dc stress at $V_{DS}=V_G=-50$ V for 25 hrs, after stress release for 1, 2, 3, 4, 5, 8, 20, 45 hrs. The BC TFT has a device feature of channel width and length of 20000 and 17 μm , respectively. (b) The square root of I_{DS} versus V_G at the same condition with (a).....**91**

Fig. 4.8 The extracted threshold voltage and mobility of the results in Fig. 4.7.....**92**

Fig. 4.9 (a) Equivalent pixel structure, including one transistor, one storage capacitor C_S and an additional assisting liquid crystal parasitic capacitor C_{LC} . The reference is made to the C_S on common pixel structure. (b) Microscopic view. (c) Cross section of active-matrix pixel structure.....**93**

Fig. 4.10 Voltage-transmittance curve of TNLC.....**94**

Fig. 4.11 A 3 inch 64×128 active-matrix TNLC display, (a) the monochrome type, (b)(c) the multi-color type with integration of color filter.....**95**

Chapter 5

Fig. 5.1 The process flow of the active-matrix CNT-FEDs.....**103-5**

Fig. 5.2 Schematic circuit and (b) layout of the novel active-matrix pixel

	structure.....	106
Fig. 5.3	(a) Schematic circuit of the discrete devices including a diode CNT-FED and a n-type TFT with feature size of channel width 8 μm and channel length 16 μm , and (b) the transfer characteristics of (a) at different anode voltage.....	107
Fig. 5.4	(a) The emission current versus voltage characteristics of diode-CNT FED that were measured from four different areas. (b) The current-voltage-brightness for a diode CNT-FED with 50 μm space distance.....	108
Fig. 5.5	Two criteria of driving TFT that were depicted by TFT's output curves along with CNT's load line.....	109
Fig. 5.6	(a) Top view of the multi-gates TFT and (b) the output characteristics of multi-gates TFT.....	110
Fig. 5.7	The transfer curves of a single gate LPTS-TFT before and after 560 $^{\circ}\text{C}$ thermal process at V_{DS} of -1 V and -10 V, respectively. The close symbol presents the case after thermal process and the open symbol denotes the origin case. The square symbol was the case at V_{DS} of -1 V, and the circle symbol was the case of V_{DS} of -10 V.....	111
Fig. 5.8	The image of 4 inch active-matrix CNTFED display driven by high voltage TFTs.....	112

